

Are there baryons which contain constituent gluons?

Eugene Golowich and Emmanuel Haqq

Department of Physics and Astronomy, University of Massachusetts, Amherst, Massachusetts 01003

Gabriel Karl

Department of Physics, University of Guelph, Guelph, Canada N1G 2W1

(Received 8 November 1982; revised manuscript received 9 March 1983)

A study of three-quark—one-gluon configurations in the zero-strangeness, positive-parity sector is carried out. The quantum numbers of the ground-state levels in this system are identified. The mass spectrum is analyzed in both the bag-model and harmonic-oscillator dynamical frameworks. Mixing between the Q^3 and Q^3G sectors is determined, and implications of Q^3 - Q^3G mixing are explored.

I. INTRODUCTION

Over a period of time there have evolved certain empirical rules governing the description of hadrons. These include associating baryons and mesons with color-singlet three-quark (Q^3) and quark-antiquark ($Q\bar{Q}$) configurations, respectively, and positing the existence of a spin-dependent potential (hyperfine interaction) to lift unwanted mass degeneracies. This “valence” picture, although undoubtedly a simplification of nature, appears to work well.^{1,2}

However, it is possible that this simple valence description might require extension. There is both experimental and theoretical evidence for the existence of (primarily) non-quark-bearing hadrons called glueballs.³⁻⁵ Moreover, just as quarks confined within hadrons seem to have characteristic energies (e.g., about 0.3 GeV per nonstrange quark) and hyperfine effects, it appears possible to employ “constituent” gluons endowed with analogous properties to generate phenomenologically acceptable glueballs. One quantitative difference is that it appears to cost more energy to add a constituent gluon to a hadron than it does a nonstrange quark.

If indeed hadrons exist which are constructed either from constituent quarks or from constituent gluons, it is natural to explore whether hybrid configurations containing some of each can occur. We have in mind not just the mixing between $Q\bar{Q}$ and gluon sectors, with each separately a color singlet, which is expected to occur at some level in the meson sector. Rather our interest is in configurations where the quark and gluon sectors are each color-bearing, yet combine to form a color-singlet hadron. Because far more is known about the zero-strangeness baryon spectrum than about hyperons or mesons of any strangeness, the most stringent test of this scenario is afforded by constructing a model of nonstrange baryons. Correspondingly then, we consider in this paper properties associated with nonstrange three-quark—one-gluon (Q^3G) configurations. We restrict our calculational study to only positive-parity ($\mathcal{P} = +$) states because these are expected to have the lowest masses.

There exist earlier studies of the excitation of gluonic

degrees of freedom in hadrons. The configuration $Q\bar{Q}G$ has been considered by Buchmüller and Tye and by Hasenfratz *et al.* for heavy b -flavored quarks, and by Barnes and Close and by Chanowitz and Sharpe for light quarks.⁶ Implementations of the Q^3G scenario using methods rather different from those considered here are carried out by Wagner and by Högaasen and Wroldsen.⁷ Preliminary descriptions of the work presented here appear in Ref. 8.

To implement our proposed program of study it is necessary to adopt a dynamical procedure. Unfortunately there does not yet exist a definitive calculational framework for quantum chromodynamics (QCD). We have employed the MIT bag model to carry out numerical calculations. Our feeling is that any such model should not be expected to provide a detailed fit to data but rather can give a reasonable picture of the anticipated Q^3G spectrum, e.g., mass splittings and relative ordering of states. We have also found it instructive to address aspects of the Q^3G system from the viewpoint of the oscillator model.

At this point we hasten to observe that Q^3G configurations are not gauge invariant. This is sometimes the case in bound-state calculations; in some formulations Q^3 configurations also are not gauge invariant. Our procedure is to adopt a particular gauge (to be defined later) and to carefully include all effects defined within that gauge.

We can of course deduce several features of Q^3G configurations which are independent of specific dynamical models. The *quantum numbers* of the Q^3G states are dictated mainly by the requirements that the three-quark sector transform as a color octet and subscribe to the constraints of Fermi-Dirac statistics. The Young tableaux associated with the color, isospin (i.e., flavor), and spin degrees of freedom are depicted in Fig. 1. For example, appearing with a spin- $\frac{3}{2}$ tableau (totally symmetric) must occur a linear combination of the color-isospin tableaux which is antisymmetric under permutation. Upon examining all possibilities we find that there are only three allowed three-quark multiplets. They have spin (S), isospin (I) values: $S = \frac{3}{2}, I = \frac{1}{2}$; $S = \frac{1}{2}, I = \frac{3}{2}$; $S = \frac{1}{2}, I = \frac{1}{2}$. Examples of each type of state expressed in terms of quark creation operators are ($\alpha = 1, \dots, 8$ is a color label)

(i) $S = \frac{3}{2}, I = \frac{1}{2}$:

$$|\frac{1}{2} \frac{3}{2}\rangle_{13}^{\alpha} = \frac{1}{12} \epsilon_{ikl} \lambda_{ji}^{\alpha} [u_i^{\dagger}(\uparrow) d_k^{\dagger}(\uparrow) u_j^{\dagger}(\uparrow) - d_j^{\dagger}(\uparrow) u_i^{\dagger}(\uparrow) u_k^{\dagger}(\uparrow)] |0\rangle; \quad (1)$$

(ii) $S = \frac{1}{2}, I = \frac{3}{2}$:

$$|\frac{3}{2} \frac{1}{2}\rangle_{31}^{\alpha} = \frac{1}{12} \epsilon_{ikl} \lambda_{ji}^{\alpha} [u_i^{\dagger}(\uparrow) u_k^{\dagger}(\downarrow) u_j^{\dagger}(\uparrow) - u_j^{\dagger}(\downarrow) u_i^{\dagger}(\uparrow) u_k^{\dagger}(\uparrow)] |0\rangle; \quad (2)$$

(iii) $S = \frac{1}{2}, I = \frac{1}{2}$:

$$|\frac{1}{2} \frac{1}{2}\rangle_{11}^{\alpha} = \frac{1}{12\sqrt{3}} \epsilon_{ikl} \lambda_{ji}^{\alpha} [-d_j^{\dagger}(\downarrow) u_i^{\dagger}(\uparrow) u_k^{\dagger}(\uparrow) - 2d_j^{\dagger}(\uparrow) u_i^{\dagger}(\uparrow) u_k^{\dagger}(\downarrow) + u_j^{\dagger}(\uparrow) u_i^{\dagger}(\uparrow) d_k^{\dagger}(\downarrow) + u_j^{\dagger}(\uparrow) u_i^{\dagger}(\downarrow) d_k^{\dagger}(\uparrow) + u_j^{\dagger}(\downarrow) u_i^{\dagger}(\uparrow) d_k^{\dagger}(\uparrow)] |0\rangle; \quad (3)$$

where our notation for state vectors is $|I_3, S_3\rangle_{2I, 2S}^{\alpha}$.

There exists an elegant way to check that we have not missed any states in our Young-tableaux construction. Taken together, the color-isospin-spin symmetries constitute an $SU(12)$ group of transformations [i.e., $SU(3) \times SU(2) \times SU(2)$]. The totally antisymmetric representation of this group (dimension 220) has $SU(3) \times SU(2) \times SU(2)$ content ${}^2_1{}^2 + {}^4_1{}^4 + {}^2_8{}^2 + {}^2_8{}^4 + {}^4_8{}^2 + {}^2_10{}^2$ where our notation is ${}^{2S+1}C^{2I+1}$, S denoting spin and C denoting color. The color-singlet states are of course just the ordinary nucleon and Δ valence composites. The three color-octet entries are precisely the structures in Eqs. (1)–(3). Finally, the color-decuplet Q^3 composite would require at least two gluons to couple to a color-singlet hadron. As such, its mass would be rather large and so we do not consider it any further in this paper.

The construction of the Q^3G configurations is completed by combining the quark and gluon sectors into a color-singlet state and coupling the Q^3 and G angular momenta in all possible ways. This results in *seven levels* in the Q^3G ground state as compared to two in the usual Q^3 valence model. The quantum numbers associated with each Q^3 and Q^3G level are enumerated in Table I. Observe that some mixing between the Q^3 and Q^3G sectors is to be expected. In particular there are two Q^3G states with the quantum numbers of the nucleon and one with the quantum numbers of the Δ . For the benefit of the reader, we list explicitly our Q^3G state vectors in the Appendix and define our notation there.

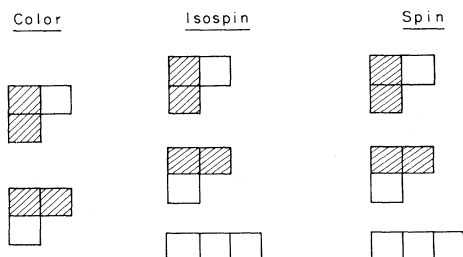


FIG. 1. Young tableaux for color-octet three-quark composite. The shaded areas indicate possible ways of assigning a given pair from the collection of three quarks in cases of mixed permutation symmetry.

Having determined the quantum numbers of the Q^3G composites, we turn to a computation of mass values and assorted mixing effects. The bag-model analysis is carried out in Sec. II. There are two subsections, II A and II B, in which we consider, respectively, mass values and then mixing effects. Section III briefly addresses the Q^3G system considered with the oscillator model and our conclusions are presented in Sec. IV.

II. Q^3G STATES IN THE BAG MODEL

A. Mass estimates

The analysis described in this section is carried out in the context of a static spherical bag of radius R . To proceed with the calculation of mass values, we specify individual contributions to the Hamiltonian, calculate the expectation value of the Hamiltonian at fixed R for the seven Q^3G states, and finally minimize each mass as a function of R .

Throughout we adopt the treatment of a confined gluon field as derived by Golowich in Ref. 9. That is, we take the time component of the gluon field to vanish and to zeroth order in the interaction, require the space component in mode n to obey (suppressing color notation)

$$[\nabla^2 + (k_n/R)^2] \vec{A}_n(x) = 0 \quad (4)$$

and

$$\vec{\nabla} \cdot \vec{A}_n(x) = 0, \quad r < R. \quad (5)$$

TABLE I. Numbers of states with definite spin and isospin for (a) Q^3 valence model and (b) Q^3G model.

Isospin	Spin		
	$\frac{1}{2}$	$\frac{3}{2}$	$\frac{5}{2}$
(a)			
$\frac{1}{2}$	1	0	0
$\frac{3}{2}$	0	1	0
(b)			
$\frac{1}{2}$	2	2	1
$\frac{3}{2}$	1	1	0

The gluon mode wave number k_n is determined by the linear relation

$$\vec{r} \times (\vec{\nabla} \times \vec{A}) = 0 \text{ at } r = R. \quad (6)$$

Because our interest lies in the Q^3G ground state, we employ throughout only the lowest positive-parity mode, for which $k = 2.7437$. This corresponds to a gluon energy roughly 50% larger than that of a quark. The gluon operator spatial dependence (for angular momentum projection λ) is given by

$$\vec{A}_\lambda(x) = N_G j_1(kr/R) \vec{X}_{1\lambda}(\Omega) a_\lambda + \text{H.c.}, \quad (7)$$

where the normalization factor N_G is given by

$$N_G^{-2} = \{3[1 - \sin(2k)/2k] - 2(1 + k^2)\sin^2 k\} R^2, \quad (8)$$

and $\vec{X}_{1\lambda}$ is a standard vector spherical harmonic.

We now list each contribution to the Hamiltonian.

(i) Quark and gluon kinetic energies:

$$H_0 = (3\omega + k)/R, \quad (9)$$

where for a quark of mass m we use $\omega \simeq 2.0428 + 0.4929mR$ for $mR \ll 1$, the situation of interest here.

(ii) Empty-bag volume energy:

$$H_1 = 4\pi R^3 B/3. \quad (10)$$

(iii) Zero-point energy:

$$H_2 = -Z_0/R. \quad (11)$$

Note, however, as shown in Ref. 10, the expectation value of H contains not only a mass contribution but also effects of bag fluctuations having roughly the form of (11). This modifies the value of Z_0 obtained originally in Ref. 1.

(iv) Coulomb energy:

$$H_3 = \frac{g^2}{2} \int d^3x \vec{E}_\alpha(x) \cdot \vec{E}_\alpha(x) \quad (12)$$

summed over the color index $\alpha = 1, \dots, 8$. This instantaneous interaction naturally separates into three parts, quark-quark, gluon-gluon, and quark-gluon. The first two of these tend to cancel against the third. The cancellation is considerable but not complete because the quark and gluon spatial wave functions differ. We find numerically

$$E_{\text{Coul}} = (0.025 + 0.114mR)\alpha_c R^{-1}, \quad (13)$$

where $\alpha_c = g^2/4\pi$ is the QCD "fine-structure constant." The Coulomb shift is rather insignificant. Incidentally, two technical matters worth noting are (a) the quark-quark Coulomb interaction includes self-energies (as in Ref. 1), and (b) because there is a clash between the spherical cavity shape and the gluon spatial behavior (7), the gluon electric field boundary constraint is not obeyed locally, but only globally.

(v) $O(\alpha_c)$ radiative corrections:

$$H_4 = H_{\text{hyp}} + H_{\text{Compt}}, \quad (14)$$

i.e., there are two classes of radiative correction, which we refer to as "hyperfine" (Fig. 2) and "Compton" (Fig. 3). Such radiative corrections are extremely important to our analysis because they lift the mass degeneracy of the seven

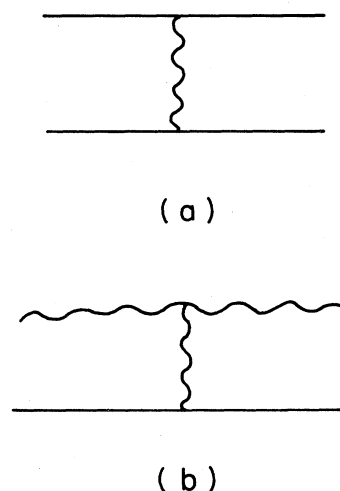


FIG. 2. QCD hyperfine interaction between (a) a pair of quarks and (b) a quark and a gluon.

Q^3G states induced by the energy contributions (i)–(iv). In view of this, let us carefully address each in turn.

That a *hyperfine* interaction should contribute to the physics of Q^3G states is not surprising given the presence of this effect in the Q^3 sector. The only significant extension is that, because gluons carry color change, we must take into account the process of Fig. 2(b) in addition to that of Fig. 2(a). Several calculational methods are available. The hyperfine effect can be computed via the expectation value

$$E_{\text{hyp}} = \left\langle Q^3G \left| -g^2 \int d^3x \vec{J}_\alpha(x) \cdot \vec{A}_\alpha^{(\text{SC})}(x) \right| Q^3G \right\rangle, \quad (15)$$

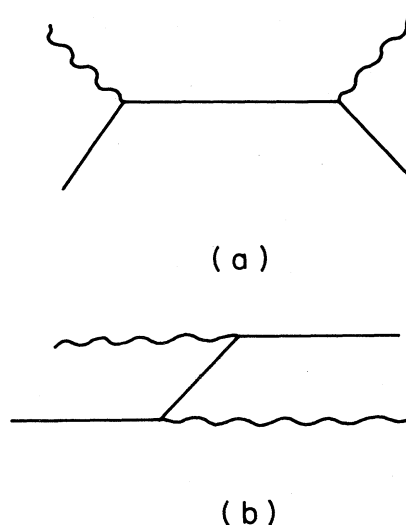


FIG. 3. QCD Compton interactions.

where $\vec{A}_\alpha^{(SC)}(x)$ is the semiclassical (SC) color vector potential associated with a quark current and \vec{J}_α is the color current density carried by both quarks and gluons. In the bag model the semiclassical vector potential has the form¹

$$\vec{A}_\alpha^{(SC)}(x) = -\frac{1}{4\pi} \frac{\lambda_\alpha}{2} \vec{r} \times \vec{\sigma} \left[\frac{\mu(r)}{r^3} + M(r) + \frac{\mu(R)}{2R^3} \right], \quad (16)$$

where

$$\mu(r) = \int_0^r dr' \mu'(r'), \quad (17)$$

$$M(r) = \int_r^R \frac{dr'}{r'^3} \mu'(r'), \quad (18)$$

and

$$\mu'(r) = 2 \left[\frac{(\omega - mR)}{(\omega + mR)} \right]^{1/2} N_{-1}^2 r^3 j_0(qr/R) j_1(qr/R). \quad (19)$$

In (19), N_{-1} is the conventional normalization factor for a bag-confined quark field, and q is the mode wave number $q = (\omega^2 - m^2 R^2)^{1/2}$. Upon multiplying \vec{A}_α by the quark color current

$$J_{k,\alpha}^{(Q)} = -\frac{1}{4\pi} \frac{\lambda_\alpha}{2} (\hat{r} \times \vec{\sigma})_k \frac{\mu'}{r^3}, \quad (20)$$

we obtain for Eq. (10) the expression

$$E_{\text{hyp}}^{(QQ)} = -(0.177 - 0.047mR) \alpha_c R^{-1} I_{QQ}, \quad (21)$$

where

$$I_{QQ} = \left\langle Q^3 G \left| \sum_{i < j} \vec{\sigma}_i \cdot \vec{\sigma}_j E_i(3) \cdot E_j(3) \right| Q^3 G \right\rangle. \quad (22)$$

In Eq. (22), we denote generators of the triplet representation of the SU(3) of color as $F_i(3)$ for quark i . The structure of $E_{\text{hyp}}^{(QQ)}$ can be understood as an overlap integral involving quark spatial wave functions [the numerical factor in Eq. (21)] times a term I_{QQ} which depends on the relative spin and color orientation of each quark pair. By exploiting the quark antisymmetry property of the $Q^3 G$ -state vector and taking account of its color and spin content, one can easily determine I_{QQ} . As an example, consider the $I = I_3 = \frac{1}{2}$, $J = J_3 = \frac{3}{2}$ level $|\frac{1}{2} \frac{3}{2}\rangle_{13}$, which arises from the Q^3 color-octet composite of Eq. (1). Noting that for this state each quark pair has spin 1 and exists on the average equally in the color representations 3^* and 6 , we deduce

$$\begin{aligned} I_{QQ} &= 3 \langle Q^3 G | \vec{\sigma}_i \cdot \vec{\sigma}_j E_i(3) \cdot E_j(3) | Q^3 G \rangle \\ &= 3 \langle \vec{\sigma}_i \cdot \vec{\sigma}_j \rangle_{S=1} \left[\frac{1}{2} \langle E_i(3) \cdot E_j(3) \rangle_{3^*} + \frac{1}{2} \langle E_i(3) \cdot E_j(3) \rangle_6 \right] = -\frac{1}{2}, \end{aligned} \quad (23)$$

and analogously for the other $Q^3 G$ levels.

We can obtain essentially the same result via second-order perturbation theory¹¹:

$$E_{\text{hyp}}^{(QQ)} = \langle Q^3 G | H'(E_0 - H_0 + i\epsilon)^{-1} H' | Q^3 G \rangle, \quad (24)$$

where H_0 is defined in Eq. (9), H' is given by

$$H' = -g \int d^3x \vec{j}_\alpha^{(Q)}(x) \cdot \vec{A}_\alpha(x), \quad (25)$$

and we interpret $\vec{A}_\alpha(x)$ as the operator of Eq. (7). There is implicit in Eq. (24) an infinite sum over all intermediate states, so the gluon propagator of Fig. 2(a) is expressible as a mode sum. In practice the sum converges quickly. Therefore, one need employ only the lowest-energy intermediate state. Let us now use this method on the quark-gluon hyperfine interaction.

To compute the process depicted in Fig. 2(b) we require the trigluon vertex

$$H'' = -\frac{g}{2} f_{\alpha\beta\gamma} A_\beta^i A_\gamma^j (\nabla^j A_\alpha^i - \nabla^i A_\alpha^j) \quad (26)$$

as well as H' of Eq. (25). Thus we use perturbation theory to write

$$E_{\text{hyp}}^{(QG)} = \langle Q^3 G | H'(E_0 - H_0 + i\epsilon)^{-1} H'' + H''(E_0 - H_0 + i\epsilon)^{-1} H' | Q^3 G \rangle. \quad (27)$$

Upon evaluating angular integrals such as

$$\int d\Omega X_{11}^i X_{11}^j (\nabla^j X_{11}^{*i} - \nabla^i X_{11}^{*j}) = \frac{1}{r} \left[\frac{3}{8\pi} \right]^{1/2} \quad (28)$$

and performing integrations over quark and gluon wave functions we obtain

$$E_{\text{hyp}}^{(QG)} = (0.244 - 0.169mR) \alpha_c R^{-1} I_{QG}, \quad (29)$$

where I_{QG} is a spin-color factor which vanishes for $I = \frac{3}{2}$ states and equals 3, 1, -2, -2, and -5, respectively, for

the $I = \frac{1}{2}$ states $|15\rangle_{13}$, $|13\rangle_{11}$, $|13\rangle_{13}$, $|11\rangle_A$, and $|11\rangle_B$.

The Compton interaction is not present in the Q^3 model; in this paper it is solely a feature of the $Q^3 G$ sector. To compute the Compton energy E_{Comp} we again employ the formulas (24) and (25) but now with respect to the processes of Figs. 3(a) and 3(b). Thus it is the quark propagators which are expressible as mode sums. Note that corresponding to each of the Figs. 3(a) and 3(b) are two time orderings, direct graphs and "Z graphs." The Z-graph amplitudes are proportional to the direct amplitudes for each of Figs. 3(a),

$$E_{\text{Comp}}^{(Z)} = 0.139E_{\text{Comp}}^{(\text{dir})}, \quad (30)$$

and 3(b),

$$E_{\text{Comp}}^{(Z)} = -0.385E_{\text{Comp}}^{(\text{dir})}. \quad (31)$$

As an example of a Compton radiative correction we write the amplitude corresponding to the direct time ordering of Fig. 3(a). Restricting the sum on intermediate states to the ground state, the amplitude can be cast in the form

$$\frac{\alpha_c}{k} \left[\frac{\omega - mR}{\omega + mR} \right] \left[2N_G N_{-1}^2 \int u^2 du j_1(ku) j_0(qu) j_1(qu) \right]^2 I, \quad (32)$$

where

$$I = \left\langle Q^3 G \left| a_{\beta, \lambda}^\dagger a_{\alpha, \lambda} q_i^\dagger \left[\frac{\lambda^\beta}{2} \frac{\lambda^\alpha}{2} \right]_{ij} q_j \left| Q^3 G \right. \right\rangle \chi^\dagger \frac{I_{\text{spin}}}{4\pi} \chi \quad (33)$$

and

$$I_{\text{spin}} = \frac{16\pi}{3} \left[\delta_{\lambda'1} \delta_{\lambda 1} \frac{(1 - \sigma_z)}{2} + \delta_{\lambda', -1} \delta_{\lambda, -1} \frac{(1 + \sigma_z)}{2} + \delta_{\lambda'0} \delta_{\lambda 0} \sigma_z \right. \\ \left. - \frac{(\sigma_x - i\sigma_y)}{2} (\delta_{\lambda'0} \delta_{\lambda, -1} + \delta_{\lambda'1} \delta_{\lambda 0}) - \frac{(\sigma_x + i\sigma_y)}{2} (\delta_{\lambda'0} \delta_{\lambda 1} + \delta_{\lambda', -1} \delta_{\lambda 0}) \right]. \quad (34)$$

One first calculates the operator matrix element of Eq. (33), which determines the quantity I_{spin} and thus the spin inner product. Clearly then, the Compton calculations although somewhat tedious are, again, straightforward.

For the degenerate $Q^3 G$ states there is an additional energy shift arising from the $\mathcal{O}(\alpha_c)$ mixings produced by the quark-gluon hyperfine and Compton graphs of Figs. 2 and 3. These mixings are nonzero between the states $|11\rangle_{11}$ and $|11\rangle_{13}$ as well as between $|13\rangle_{11}$ and $|13\rangle_{13}$. From perturbation theory, the energy shift for two degenerate states $|i\rangle$ and $|j\rangle$ is

$$\delta E_{\pm} = \frac{1}{2} (\langle i | H | i \rangle + \langle j | H | j \rangle) \pm \frac{1}{2} [(\langle i | H | i \rangle - \langle j | H | j \rangle)^2 - 4 |\langle i | H | j \rangle|^2]^{1/2}.$$

The calculation of the diagonal matrix elements has been described above. The off-diagonal elements may also be calculated without difficulty using the mode sum approach; we obtain the rather small values

$$\begin{aligned} {}_{11}\langle 11 | H^2 | 11 \rangle_{13} &= -0.02 \frac{\alpha_c}{R}, \\ {}_{11}\langle 13 | H^2 | 13 \rangle_{13} &= -0.009 \frac{\alpha_c}{R}, \end{aligned} \quad (35)$$

where H^2 symbolizes the hyperfine and Compton interactions. It is evident that the off-diagonal matrix elements make a negligible contribution to the energy shifts of these states.

This completes the presentation of terms appearing in the Hamiltonian. It is instructive at this point to refer to Table II where we list in units of R^{-1} certain contributions to the energy of both Q^3 and $Q^3 G$ states. For definiteness the quark mass is fixed at the value zero. We do not exhibit H_1 or H_2 of Eqs. (10) and (11) in Table II because each depends on a quantity (Z_0 and B) to be determined by our fitting procedure. The most apparent property of Table II is the large size of kinetic-energy contributions relative to all others. That the mass of a light hadron is mainly attributable to constituent kinetic energy is a common feature of bag models. It clearly generalizes to the $Q^3 G$ states. In potential models, the "constituent mass" plays this role. Another noteworthy aspect of Table II is the very large, negative quark-gluon hyperfine interaction for the $I=J=\frac{1}{2}$ $Q^3 G$ state $|11\rangle_A$. Indeed if the Compton radiative correction were not present, the

mass of the $|11\rangle_A$ state would be unacceptably low. Thus an interaction (e.g., Compton or something like it) distinct from the hyperfine interaction of the Q^3 model *must* be present in the $Q^3 G$ model if it is to make any sense.

There are several parameters in our formulas—the quark mass m , bag constant B , zero-point constant Z_0 , the radius R for each level, and the QCD fine-structure constant α_c . Although there has been recent work on the origin of bag parameters,¹²⁻¹⁴ standard usage is employed here. We incorporate the momentum dependence of α_c by employing the parametrization of Ref. 10,

$$\alpha_c(R) = \frac{2\pi}{9} \frac{1}{\ln(A + R_0/R)}. \quad (36)$$

To fix these parameters we employ the N, Δ mass values, impose the constraint that the pion mass vanish as the quark mass does, require for each level of mass M that $dM(R)/dR=0$, and as in Ref. 10, use perturbation theory about $m=0$ to relate the pion and quark masses. In the latter step our results differ somewhat from Ref. 10 due to a more careful treatment of the hyperfine overlap integral. This procedure still leaves some freedom in the choice of one parameter, e.g., A of Eq. (35). To obtain some feeling for the sensitivity of the computed quantities to the parametrization, we present our numerical analysis for $A=1.0$ and 0.9 .¹⁰ Another aspect of the calculation, which in our opinion is somewhat a matter of taste, is whether to express the baryon bag energy relativistically as $(M^2 + \langle p^2 \rangle R^{-2})^{1/2}$ or nonrelativistically as $M + \langle p^2 \rangle / 2MR^2$. We list results for each choice. Our find-

TABLE II. Energy contributions to Q^3 and Q^3G states. The common energy unit is R^{-1} . The quark mass equals zero here. The Compton entries (a) and (b) refer, respectively, to the processes depicted in Figs. 3(a) and 3(b). Each Coulomb, hyperfine, and Compton entry is to be multiplied by α_c .

		Kinetic	Coulomb	Hyperfine		Compton	
				$Q-Q$	$Q-G$	(a)	(b)
Q^3	N	6.128	0	-0.354			
	Δ	6.128	0	0.354			
Q^3G	$ 15\rangle_{13}$	8.872	0.025	0.089	0.732	0	0.108
	$ 33\rangle_C$	8.872	0.025	0.443	0	0.268	0.090
	$ 13\rangle_{11}$	8.872	0.025	-0.089	0.244	0.134	0.072
	$ 13\rangle_{13}$	8.872	0.025	0.089	-0.488	0.334	0.018
	$ 11\rangle_B$	8.872	0.025	-0.089	-0.488	0.334	0.018
	$ 31\rangle_{31}$	8.872	0.025	0.443	0	0.067	-0.018
	$ 11\rangle_A$	8.872	0.025	0.089	-1.220	0.536	-0.036

ings are presented in Tables III and IV and Fig. 4. We defer discussion of these to the Conclusion. However, we note here that the maximum scatter associated with the different approaches is roughly 30 MeV.

B. Mixing effects

Our original Q^3G basis is listed in the Appendix. QCD interactions cause mixings between the Q^3 and Q^3G states as well as among the Q^3G states. The original basis, diagonal in the kinetic energy, is thus altered.

In the Q^3G sector, as discussed in Sec. IIA, the Compton and hyperfine interactions produce mixings between $|11\rangle_{11}$ and $|11\rangle_{13}$ as well as between $|13\rangle_{11}$ and $|13\rangle_{13}$. These mixings are small. Call δ the $O(\alpha_c)$ energy shift difference between degenerate pairs of states obtained, for example, from Table II. Then the mixing is governed by the ratio of the (rather small) matrix element of Eq. (35) to δ . For example, we find

$$|11\rangle_{11} \rightarrow (1 - \epsilon^2)^{1/2} |11\rangle_{11} + \epsilon |11\rangle_{13}, \quad (37)$$

where $\epsilon \sim 0.05$. The size of the matrix elements of Eq. (35) thus guarantees that mixings among the Q^3G states are small. In what follows we therefore neglect these mixing effects and simply employ our original basis of Q^3G state vectors.

Mixing between the Q^3 and Q^3G sectors is, however, significant. The two $I=J=\frac{1}{2}$ and one $I=J=\frac{3}{2}$ mixings are describable in terms of a common amplitude $-1.39i\sqrt{\alpha_c}$, as generated in Fig. 5(a). Our notation for the mixed states is $|P\rangle, |11\rangle_A, |11\rangle_B$ and $|\Delta\rangle, |33\rangle_C$.

These evolve, respectively, into the unmixed states $|11\rangle_{Q^3}, |11\rangle_{11}, |11\rangle_{13}$ and $|33\rangle_{Q^3}, |33\rangle_{31}$ in the limit $\alpha_c \rightarrow 0$. In particular, the nucleon and Δ Q^3 - Q^3G mixed state vectors take the form to first order in g ,

$$|\Delta^{++}\rangle = (1 - \eta^2)^{1/2} |\Delta^{++}\rangle_{Q^3} - i\eta |33\rangle_{31}, \quad (38)$$

$$|P\rangle = \left[\frac{1 - \eta^2}{2} \right]^{1/2} |P\rangle_{Q^3} - i\eta (|11\rangle_{13} + |11\rangle_{11}) \quad (39)$$

with

$$\eta = \frac{1.39\sqrt{\alpha_c}}{E_G}, \quad (40)$$

where $E_G = 2.7437 + \text{self-energy effects}$. For zero gluon self-energy the mixing is appreciable, $\eta = 0.59$. Even if the gluon self-energy is large, the mixing might still be non-negligible because N - Δ splitting fixes the value of α_c/E_G .

Before considering the effect of Q^3 - Q^3G mixing on proton observables, we briefly address for pedagogical reasons the procedure by which the Hamiltonian is diagonalized. There are some pitfalls in obtaining mass values via the diagonalization procedure of which we have found some researchers to be unaware.

For definiteness consider mixing of the two $I=J=\frac{3}{2}$ states. Upon diagonalizing the Hamiltonian, one must expand the resulting mass values to $O(\alpha_c)$ for reasons of consistency. Thus the $I=J=\frac{3}{2}$ mass matrix

TABLE III. Variation of parameters. Entries for quark mass m and bag constant $B^{1/4}$ are in units of GeV, whereas R_0 has unit GeV^{-1} . Parameter A is defined in Eq. (36) and the labels Rel and NR refer to treating the baryon bag energy relativistically or nonrelativistically.

	A	m	$B^{1/4}$	Z_0	R_0
Rel	1.0	0.025	0.138	1.02	2.23
Rel	0.9	0.025	0.140	1.10	2.77
NR	1.0	0.024	0.142	1.07	2.35
NR	0.9	0.024	0.144	1.14	2.88

TABLE IV. Variation of Q^3G masses. All masses are given in units of GeV. Energy contributions up to $O(\alpha_c)$ are included but self-energy contributions to quarks and gluons are not.

	A	$ 15\rangle_{13}$	$ 33\rangle_C$	$ 13\rangle_{11}$	$ 13\rangle_{13}$	$ 11\rangle_B$	$ 31\rangle_{31}$	$ 11\rangle_A$
Rel	1.0	1.930	1.910	1.740	1.613	1.549	1.787	1.420
Rel	0.9	1.952	1.931	1.755	1.624	1.557	1.804	1.425
NR	1.0	1.944	1.923	1.760	1.636	1.573	1.805	1.447
NR	0.9	1.965	1.942	1.774	1.647	1.582	1.821	1.453

$$\begin{pmatrix} A & i\sqrt{\alpha_c}B \\ -i\sqrt{\alpha_c}B & C + D\alpha_c \end{pmatrix} \quad (41)$$

yields the mass eigenstates

$$\lambda_+ = C + \alpha_c \left[D + \frac{B^2}{C-A} \right], \quad (42)$$

$$\lambda_- = A - \alpha_c \frac{B^2}{C-A}.$$

First note that in (42), one must be careful not to include as diagonal contributions those energy shifts which are in-

duced via the diagonalization procedure [e.g., as in Fig. 5(b)]. To do so would amount to double counting. Even if the calculation is performed correctly up to this point, the mass values λ_{\pm} are not yet in useful form. The mass λ_- contains a renormalization contribution (equaling $-1.06\alpha_c$) which must be subtracted off. Also, the mass value λ_+ has a contribution, induced as in Fig. 5(c), which is canceled by its time-ordered counterpart. This latter number (equaling $-0.47\alpha_c$) must be independently calculated, a task which was not necessary in our analysis of Sec. II A.

To determine the effect of Q^3 - Q^3G mixing on proton observables, we compute the matrix element

$$\begin{aligned} \langle P \uparrow | q_i^\dagger(1)q_i(2) | P \uparrow \rangle &= \frac{|\eta|^2}{3} [\delta_{qu}(5\delta_{1\uparrow}\delta_{2\uparrow} + \delta_{1\downarrow}\delta_{2\downarrow}) + \delta_{qd}(\delta_{1\uparrow}\delta_{2\uparrow} + 2\delta_{1\downarrow}\delta_{2\downarrow})] \\ &+ \frac{1-|\eta|^2}{18} [\delta_{qu}(26\delta_{1\uparrow}\delta_{2\uparrow} + 10\delta_{1\downarrow}\delta_{2\downarrow}) + \delta_{qd}(7\delta_{1\uparrow}\delta_{2\uparrow} + 11\delta_{1\downarrow}\delta_{2\downarrow})] \end{aligned} \quad (43)$$

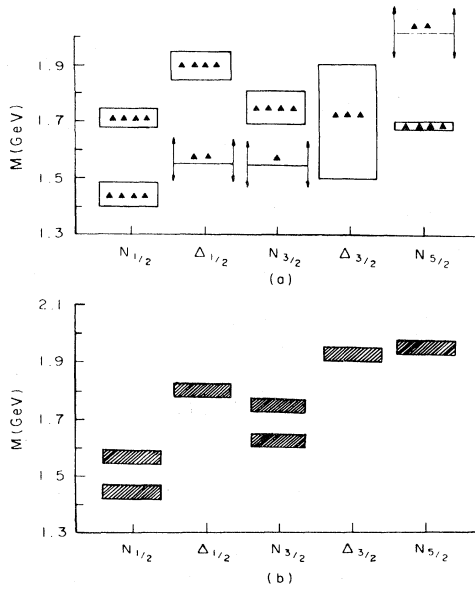


FIG. 4. Comparison between (a) experimental and (b) predicted Q^3G spectra. In (a), the number of solid triangles indicates the quality of the experimental data. Those states which are not well established in (a) have indefinite upper and lower mass estimates. Quark and gluon self-energies are not included in (b).

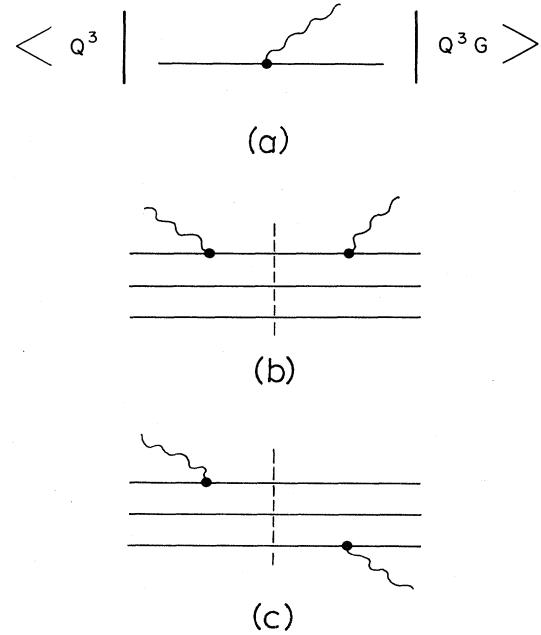


FIG. 5. Mixing effects: the amplitude connecting Q^3 and Q^3G states is depicted in (a) and energy contributions to Q^3G levels as induced by diagonalization of the mass matrix are shown in (b) and (c).

and observe that the axial-vector coupling constant, magnetic moment, and electromagnetic charge radius depend, respectively, on the expectation values of $\sigma_3\tau_3$, $Q\sigma_3$, and Q , where Q is the electric charge. Thus we find

$$\begin{aligned} g_A &= \frac{2+\eta^2}{3} g_A(Q^3), \\ \mu &= \frac{2+\eta^2}{3} \mu(Q^3), \\ \langle r^2 \rangle_{EM} &= \langle r^2 \rangle_{EM}(Q^3). \end{aligned} \quad (44)$$

The effect of mixing with the Q^3G states is seen to decrease the proton value of g_A and μ relative to their value in the Q^3 model while leaving $\langle r^2 \rangle_{EM}$ unchanged. Our result for g_A is in accord with that obtained some time ago by Golowich in Ref. 9.

Finally, recall that the Q^3 model supports a set of positive-parity radially excited states. The Q^3G ground states will mix with these Q^3 radially excited states as well as with the Q^3 ground state. We find that to $O(g)$ the $I=J=\frac{1}{2}$ and $I=J=\frac{3}{2}$ radially excited states mix with the Q^3G states with a common amplitude $-0.107i\sqrt{\alpha_c}R^{-1}$. Thus the $Q^2Q^*-Q^3G$ mixing amplitude is 7.7% that of Q^3-Q^3G . Even with the smaller $Q^2Q^*-Q^3G$ energy denominators, it would appear that $Q^2Q^*-Q^3G$ mixing is not of dominant importance.

III. Q^3G STATES IN THE HARMONIC-OSCILLATOR MODELS

It is instructive to compare aspects of the bag-model calculation just performed with the harmonic-oscillator approach. In the latter we represent the constituent gluon by a massive spin-1 particle and include as usual three massive quarks of spin $\frac{1}{2}$. The gluon mass is not predicted in the oscillator model; instead it must be supplied from another source (such as the bag model where we have seen $m \simeq 600$ MeV).

To estimate the effect of hyperfine interactions between quarks, and also between quarks and the gluon on the Q^3G manifold of states is not difficult. A simple estimate, sufficient for an initial try, is afforded by taking the quark-quark hyperfine interaction to be the same as for Q^3 baryons and normalizing the quark-gluon interaction analogously, viz.,

$$H_{qG}^{\text{hyp}} = C \langle \underline{E}_q \cdot \underline{E}_G \rangle \langle \vec{S}_q \cdot \vec{S}_G \rangle \langle \delta^3(\vec{r}_{qG}) \rangle, \quad (45)$$

where C can be normalized from the N - Δ splitting

$$\begin{aligned} C \langle \delta^3(\vec{r}_{qG}) \rangle_{Q^3G} &= C \langle \delta(\vec{r}_{qq}) \rangle_{Q^3} \\ &\simeq 300 \text{ MeV}. \end{aligned} \quad (46)$$

We could improve our estimate by making a more detailed oscillator model for the Q^3G system and estimating the wave function at zero quark-gluon separation.

Equation (45) provides an easy check on some of the results of Sec. II. The quantity $\langle \underline{E}_q \cdot \underline{E}_G \rangle$ is either $-\frac{1}{2}$ or $-\frac{3}{2}$ for the "spectator" diquark color representation 6 or $\bar{3}$, respectively. The spin expectation value involves the total angular momentum J of the Q^3G state. For example, in the spin-quartet states $S = \frac{3}{2}$, we have

$$\langle \vec{S}_3 \cdot \vec{S}_G \rangle = [J(J+1) - \frac{23}{4}] / 6$$

so that

$$\begin{aligned} \langle \frac{1}{2} \frac{3}{2} | 3H_{qG} | \frac{1}{2} \frac{3}{2} \rangle &= -\frac{1}{2} [J(J+1) - \frac{23}{4}] C \langle \delta^3(\vec{r}_{qG}) \rangle, \\ \langle \frac{1}{2} \frac{1}{2} | 3H_{qG} | \frac{1}{2} \frac{1}{2} \rangle &= -\frac{1}{2} [J(J+1) - \frac{11}{4}] C \langle \delta^3(\vec{r}_{qG}) \rangle, \end{aligned} \quad (47)$$

whereas the corresponding matrix element for the $I = \frac{3}{2}$, $J = \frac{1}{2}$ sector vanishes.

It is not obvious how to obtain a meaningful nonrelativistic estimate for the Compton amplitudes. The heavy interacting particles of the oscillator model would have to be created or destroyed as in Figs. 2(a) and 2(b). In this regard the nonrelativistic approach would appear to be lacking unless some correspondence with these processes could be constructed.

IV. CONCLUSION AND SUMMARY

In this paper we have seriously entertained the possibility that "constituent" or "valence" gluonic degrees of freedom exist within baryons. Our motivation arose mainly from theoretical and experimental evidence for glueball states.

Baryonic excitations have traditionally provided a rich arena for experimental study. At present their study is also a subject of intense theoretical activity. Indeed, there have been very recent works suggesting the existence of hadron surface modes,¹⁵ constituent gluon modes,¹⁶ and even one suggesting that such excitations are inconsistent with the baryon spectrum for masses lighter than 2.5 GeV.¹⁷

Our specific aim has been to compute Q^3G masses to $O(\alpha_c)$ and to determine mixing effects at a level consistent with our mass analysis. Throughout, the parametrization has been chosen to closely resemble that employed in earlier, successful phenomenology. We have found mass values of pure and mixed Q^3G states in the range 1.42–1.95 GeV (see Table IV and Fig. 4). In addition we have shown that a Q^3G component in the proton serves to lower the axial-vector coupling constant and magnetic moment relative to their Q^3 values but leaves the electromagnetic charge radius unchanged.

What can be inferred from these results? Because our calculation does not by itself provide an all-encompassing test of the Q^3G scenario, it would be premature and even naive at this time to draw overly firm conclusions. For example, corrections to proton observables other than those considered here are possible.¹⁸ Thus it seems prudent to instead consider each of several possible interpretations.

The Q^3G model, unadorned by gluon self-energy effects and/or QCD perturbations of higher order, has a light $J=T=\frac{1}{2}$ level which one is tempted to associate with the Roper resonance $N'(1470)$. However, the radially excited Q^3 model is usually invoked to explain this state. There is a possible resolution to this dilemma. From time to time, there have been claims that two quasidegenerate states appear in the Roper region.¹⁹ It is not inconceivable therefore that both Q^3G and Q^2Q^* levels exist. Unfortunately

this scenario has a severe difficulty. It would imply that a number of quasidegenerate Q^3G , Q^2Q^* levels occur. This is not in accord with experiment, unless perhaps the Q^3G states are decoupled from the two-body channels on which resonance assignments are largely based. Evidently an investigation of the Q^3G decay amplitudes, say along the lines of Ref. 20, is called for. If so it would be advisable to have fairly precise wave functions, containing even $O(\alpha_c)$ mixing effects.

Another possibility is that the Q^2Q^* and Q^3G models are complementary in that they are alternative ways of explaining the same states. This is evidently not possible in the meson sector where the $Q\bar{Q}G$ spectrum contains a state ($J^{PC}=1^{-+}$) which cannot occur in the $Q\bar{Q}$ model. If Q^2Q^* , Q^3G complementarity were valid, it should be possible to demonstrate it explicitly. Perhaps the QCD equations of motion for coupled quarks and gluons along with appropriate interpolating Q^3 and Q^3G fields could accomplish this.

Finally, assume in the following that neither of the aforementioned scenarios is correct. Then given that the very concept of constituent gluon makes sense and that our phenomenological models are not totally inadequate, we are left with the option of extending our approach in some manner. Two potentially important effects are higher-order QCD corrections and constituent gluon self-energy. The former has been suggested (via box diagrams) as a significant contributor in resolving the mesonic $U(1)$ problem.²¹ The latter has been used to fit the $Q\bar{Q}G$ model to the 0^{-+} state $\iota(1440)$.^{6,14} If both mechanisms are important, then any fit which omits one or the other is of course suspect. Also, there is no *a priori* guarantee as to the magnitude or even sign of the net energy shift. It must be calculated. At any rate, such effects have at least the potential for substantially increasing the energy needed to excite Q^3G levels. This could explain the negative results obtained thus far regarding $b\bar{b}G$ states.²²

Our work suggests several further avenues of investigation. Calculation of Q^3G decay widths, gluon self-energy, higher-order QCD interactions, and clarification of Q^2Q^* - Q^3G complementarity are each matters of some importance. Work on them is underway.

ACKNOWLEDGMENTS

This research was supported in part by the National Science Foundation and by the Natural Sciences and Engineering Research Council of Canada. The authors glad-

ly acknowledge useful conversations with S. Brodsky, M. Chanowitz, J. Cornwall, J. Donoghue, R. Jaffe, N. Isgur, and an informative communication from F. Close. One of us (E.G.) thanks Brookhaven National Laboratory for hospitality during the final stages of the calculation described herein.

APPENDIX

We list below in terms of products of three-quark and gluon-state vectors the state of highest weight for each of the seven Q^3G levels. We label the gluon states in terms of spin alignment λ and color α , viz., $|\lambda\rangle^\alpha$, and the three-quark states with the notation of Eqs. (1)–(3). Denoting the color-singlet Q^3G angular momentum by J , the Q^3 spin as S , and hence each color singlet Q^3G by $|I_3, J_3\rangle_{2I, 2S}$, we have (the color index $\alpha=1, \dots, 8$ is summed over)

$$(i) J = \frac{5}{2},$$

$$|\frac{1}{2} \frac{5}{2}\rangle_{13} = |1\rangle^\alpha |\frac{1}{2} \frac{3}{2}\rangle_{13}^\alpha; \quad (A1)$$

$$(ii) J = \frac{3}{2},$$

$$|\frac{1}{2} \frac{3}{2}\rangle_{13} = (\frac{3}{5})^{1/2} |0\rangle^\alpha |\frac{1}{2} \frac{3}{2}\rangle_{13}^\alpha$$

$$- (\frac{2}{5})^{1/2} |1\rangle^\alpha |\frac{1}{2} \frac{1}{2}\rangle_{13}^\alpha, \quad (A2)$$

$$|\frac{3}{2} \frac{3}{2}\rangle_{31} = |1\rangle^\alpha |\frac{3}{2} \frac{1}{2}\rangle_{31}^\alpha, \quad (A3)$$

$$|\frac{1}{2} \frac{3}{2}\rangle_{11} = |1\rangle^\alpha |\frac{1}{2} \frac{1}{2}\rangle_{11}^\alpha; \quad (A4)$$

$$(iii) J = \frac{1}{2},$$

$$|\frac{1}{2} \frac{1}{2}\rangle_{13} = (\frac{1}{2})^{1/2} |-1\rangle^\alpha |\frac{1}{2} \frac{3}{2}\rangle_{13}^\alpha$$

$$- (\frac{1}{3})^{1/2} |0\rangle^\alpha |\frac{1}{2} \frac{1}{2}\rangle_{13}^\alpha$$

$$+ (\frac{1}{6})^{1/2} |1\rangle^\alpha |\frac{1}{2} - \frac{1}{2}\rangle_{13}^\alpha, \quad (A5)$$

$$|\frac{3}{2} \frac{1}{2}\rangle_{31} = (\frac{2}{3})^{1/2} |1\rangle^\alpha |\frac{3}{2} - \frac{1}{2}\rangle_{31}^\alpha$$

$$- (\frac{1}{3})^{1/2} |0\rangle^\alpha |\frac{3}{2} \frac{1}{2}\rangle_{31}^\alpha, \quad (A6)$$

$$|\frac{1}{2} \frac{1}{2}\rangle_{11} = (\frac{2}{3})^{1/2} |1\rangle^\alpha |\frac{1}{2} - \frac{1}{2}\rangle_{11}^\alpha$$

$$- (\frac{1}{3})^{1/2} |0\rangle^\alpha |\frac{1}{2} \frac{1}{2}\rangle_{11}^\alpha. \quad (A7)$$

QCD interactions produce Q^3 - Q^3G and Q^3G - Q^3G mixings as described in Sec. II B.

¹T. DeGrand, R. Jaffe, K. Johnson, and J. Kiskis, Phys. Rev. D **12**, 2060 (1975).

²N. Isgur and G. Karl, Phys. Rev. D **19**, 2653 (1979).

³For discussion and analysis of experimental data, see D. Scharre, invited talk at Orbis Scientiae, Coral Gables, Florida 1982 (unpublished); J. F. Donoghue, invited talk at 21st International Conference on High Energy Physics, Paris, 1982 (unpublished); E. Bloom, rapporteur's talk at 21st International Conference on High Energy Physics, Paris, 1982 (unpublished).

⁴For phenomenologically oriented theoretical analyses, see J. F. Donoghue, K. Johnson, and B. A. Li, Phys. Lett. **99B**, 416 (1981); C. Carlson, J. J. Coyne, P. Fishbane, F. Gross, and S. Meshkov, *ibid.* **99B**, 353 (1981); M. Chanowitz, in *Particles and Fields—1981: Testing the Standard Model*, proceedings of the Meeting of the Division and Particles and Fields of the APS, Santa Cruz, California, edited by C. Heusch and W. T. Kirk (AIP, New York, 1982).

⁵For QCD lattice calculations, see R. Brower, M. Creutz, and M. Nauenberg, Nucl. Phys. **B210**, 133 (1982); B. Berg and A.

- Billoire, Phys. Lett. **114B**, 324 (1982); K. Ishikawa, M. Teper, and G. Schierzholz, *ibid.* **110B**, 399 (1982); **116B**, 429 (1982).
- ⁶W. Buchmüller and S.-H. H. Tye, Phys. Rev. Lett. **44**, 850 (1980); P. Hasenfratz, R. R. Horgan, J. Kuti, and J. M. Richard, Phys. Lett. **95B**, 299 (1980); Ted Barnes and F. E. Close, Rutherford Report No. RL-82-037, 1982 (unpublished); M. Chanowitz and S. Sharpe, Lawrence Berkeley Report No. LBL 14865, 1982 (unpublished).
- ⁷F. Wagner, in *New Flavors and Hadron Spectroscopy*, proceedings of the XVIIth Rencontre de Moriond, Les Arcs, France, 1981 edited by J. Trân Thanh Vân, (Editions Frontières, Dreux, France, 1981); H. Högaasen and J. Wroldsen, LAPP Report No. Th-57, 1982 (unpublished).
- ⁸E. Golowich and E. Haqq, Bull. Am. Phys. Soc. **27**, 458 (1982); G. Karl, contribution to LAMPF II Workshop (unpublished).
- ⁹E. Golowich, Phys. Rev. D **18**, 927 (1978).
- ¹⁰J. F. Donoghue and K. Johnson, Phys. Rev. D **21**, 1975 (1980).
- ¹¹For a calculation of this type see, e.g., F. E. Close and R. R. Horgan, Nucl. Phys. **B164**, 413 (1980); **B185**, 333 (1981).
- ¹²T. H. Hansson and R. L. Jaffe, MIT Report No. CTP 1026, 1982 (unpublished). Also see C. Peterson, T. H. Hansson, and K. Johnson, Phys. Rev. D **26**, 415 (1982).
- ¹³K. Milton, Oklahoma State Research Note No. 136, 1982 (unpublished).
- ¹⁴T. H. Hansson, K. Johnson, and C. Peterson, Phys. Rev. D **26**, 2069 (1982); C. E. Carlson, T. H. Hansson, and C. Peterson, Phys. Rev. D **27**, 1556 (1983).
- ¹⁵P. J. Mulders, Bhamathi, L. Heller, A. T. Aerts, and A. K. Kerman, Phys. Rev. D **27**, 2708 (1983); G. E. Brown, J. W. Durso, and M. B. Johnson, Stony Brook report, 1982 (unpublished).
- ¹⁶T. Barnes and F. E. Close, Rutherford Report No. RL-82-110, 1982 (unpublished). This work contains considerable overlap with the one described here.
- ¹⁷R. K. Bhaduri and M. Dey, McMaster report, 1982 (unpublished).
- ¹⁸For example, QCD sea corrections are given in J. F. Donoghue and E. Golowich, Phys. Rev. D **15**, 3421 (1977).
- ¹⁹Most recently, see V. A. Gordeev *et al.*, Nucl. Phys. **A364**, 408 (1981).
- ²⁰R. Koniuk and N. Isgur, Phys. Rev. D **21**, 1868 (1980).
- ²¹J. F. Donoghue and H. Gomm (unpublished).
- ²²M. G. D. Gilchriese, Cornell report, 1982 (unpublished). See also Ref. 16 for mention of light $\bar{Q}Q$ phenomenology.